PHYSICAL REVIEW C **75**, 015202 (2007)

Quark-hadron duality in neutrino scattering

O. Lalakulich,[1] W. Melnitchouk,[2] and E. A. Paschos[1]
[1]*Universität Dortmund, Institut für Physik, D-44221 Dortmund, Germany*
[2]*Jefferson Lab, 12000 Jefferson Avenue, Newport News, Virginia 23606, USA*
(Received 17 August 2006; published 5 January 2007)

We present a phenomenological model of the quark-hadron transition in neutrino-nucleon scattering. Using recently extracted weak nucleon transition form factors, we investigate the extent to which local and global quark-hadron duality is applicable in the neutrino F_1, F_2, and F_3 structure functions and contrast this with duality in electron scattering. Our findings suggest that duality works relatively well for neutrino-nucleon scattering for the F_2 and F_3 structure functions but not as well for F_1. We also calculate the quasielastic, resonance, and deep inelastic contributions to the Adler sum rule and find it to be satisfied to within 10% for $0.5 \lesssim Q^2 \lesssim 2$ GeV^2.

DOI: 10.1103/PhysRevC.75.015202 PACS number(s): 25.30.Pt, 13.15.+g, 14.20.Gk

I. INTRODUCTION

Historically, neutrino scattering has provided vital information on the structure of the nucleon, complementary to that obtained by the more ubiquitous electromagnetic probes. In deep inelastic scattering (DIS), neutrino-induced structure functions have been used, in conjunction with electromagnetic structure functions, as the primary tool to separate valence and sea quark distributions. Neutrinos are also necessary to complete our knowledge of the full vector and axial vector structure of the nucleon elastic and transition form factors.

At the parton level, deep inelastic structure functions describe incoherent scattering of a hard probe from quarks and gluons (generically, partons) in the nucleon; form factors, in contrast, characterize the coherent or bound-state response of the nucleon to an electromagnetic or weak probe. Although on the face of it the physics of coherent and incoherent processes is rather distinct, they are in fact intimately related through the phenomenon of quark-hadron duality.

Quark-hadron duality in structure functions refers to the observation, first made by Bloom and Gilman [1], that the average over resonances produced in inclusive eN scattering closely resembles the leading twist (or "scaling") function measured in the deep inelastic region. Furthermore, as Q^2 increases the average over resonances approaches the asymptotic scaling function. Within quantum chromodynamics (QCD), the degree to which this "Bloom–Gilman duality" holds is a direct reflection of the size of higher twist effects in the nucleon [2,3]. According to the operator product expansion (OPE), higher twists are related to nucleon matrix elements of multiquark or quark-gluon operators, which contain information on long-range, nonperturbative interactions between partons. Such interactions characterize the structure of the resonances and diminish with powers of $1/Q^2$ as $Q^2 \to \infty$.

Recently there has been a resurgence of interest in duality in electron scattering at Jefferson Lab (JLab) and elsewhere, where its target, flavor, spin, and nuclear dependence have been explored [4–12]. Duality has been confirmed to good accuracy for the proton F_2 and F_L structure functions to Q^2 values as low as 1 GeV^2 or even lower. The basic features of duality have also been studied in terms of dynamical models [13–15], in phenomenological parametrizations of the form factors [16–18], as well as in the Rein-Sehgal model [19] and (in the Δ-resonance region) the Sato-Lee model [20].

Within the models, neutrino scattering can provide an important consistency check and lead to a better understanding of the systematics of nucleon $N \to$ resonance R transitions. Although the phenomenological information on duality from electron scattering has been steadily accumulating [21], there is at present almost nothing known empirically about the workings of duality in neutrino scattering. There are plans, however, to measure neutrino cross sections using a high-intensity neutrino beam at Fermilab [22].

In a parallel development, recent theoretical work has investigated the excitation of resonances by neutrinos for both $J = 3/2$ [23,24] and $J = 1/2$ resonances [25]. In the latter work the weak vector form factors were determined from Jefferson Lab data using the conserved vector current (CVC) hypothesis and two of the axial form factors from partial conservation of the axial current (PCAC), although the Q^2 dependence was not very well constrained. To date there are only rudimentary data on neutrino production of resonances beyond the $P_{33}(1232)$ region; however, more accurate data are expected, and a precise comparison will be possible in the future. In this article we use the recent theoretical results to perform a detailed phenomenological study of duality in neutrino scattering.

If one assumes that duality holds for neutrino scattering, then the average area under the resonances must follow the scaling curve. In this case the results of our comparison can be interpreted as a check on how well the Q^2 dependence of the transition amplitudes $N \to R$ is known. Deviations from duality would in this case provide information on the size of the background, and of the axial form factors, which were not determined in the model [25] for example, the normalization of C_3^A and C_4^A for the $D_{13}(1520)$ resonance, as well as the Q^2 dependence of all axial form factors]. Obtaining a better understanding of the dynamics in this kinematic region is also crucial for the interpretation of neutrino-oscillation experiments [26].

In Sec. II we review the formalism used in this study and provide details about the transition form factor parametrizations. In Sec. III, results on local and global aspects of duality in

neutrino scattering are discussed and contrasted with duality in electron scattering. We also discuss the saturation of the Adler sum rule, including its contributions from resonances and quasielastic and DIS regions. Finally, in Sec. IV we summarize our results and draw conclusions from our study.

II. FORMALISM

Testing the degree to which duality in lepton-nucleon scattering is valid requires knowledge both of structure functions in the resonance region and of the scaling functions applicable in the DIS regime. The former are calculated in terms of the nucleon $\to$ resonance transition form factors, whereas the latter can be evaluated from twist-two parton distribution functions. In this section we review both of these inputs, first outlining the parametrizations of the $N \to R$ transition form factors from which the resonance structure functions are computed and then summarizing the essential formulas for the twist-two structure functions. A more complete account of the formalism can be found in Refs. [24,25]; here we present only those details that are pertinent to the specific discussion of duality.

A. Weak transition form factors

In recent work by the Dortmund group, neutrino production of the $P_{33}(1232)\Delta$ resonance [23,24] was extended to cover also the second resonance region [25], which includes three isospin-1/2 resonances: the $P_{11}(1440)$ Roper resonance and the two negative-parity states $D_{13}(1520)$ and $S_{11}(1535)$. In the following we summarize the weak transition form factors for these resonances. The definitions and notations for the cross sections and transition form factors are taken from Eqs. (IV.12)–(IV.15) and (IV.26)–(IV.28) in Ref. [25].

1. $P_{33}(1232)$ resonance

Historically, the $P_{33}(1232)(\Delta)$ isobar has been studied more extensively than any other nucleon resonance. Electroproduction data on differential and integrated cross sections have been used to extract the $N \to \Delta$ transition form factor, and the resulting vector form factors, in the region $Q^2 < 3.5$ GeV^2, and can be parametrized (in the notation of Ref. [25]) as

$$C_3^{(p)} = \frac{2.13 D_V}{1 + Q^2/4M_V^2}, \quad C_4^{(p)} = \frac{-1.51 D_V}{1 + Q^2/4M_V^2}, \quad C_5^{(p)} = \frac{0.48 D_V}{1 + Q^2/0.776 M_V^2}, \tag{1}$$

where $D_V = 1/(1 + Q^2/M_V^2)^2$ is the dipole function with the vector mass parameter $M_V = 0.84$ GeV and the superscript (p) denotes a proton target. From isospin invariance, the electroproduction amplitudes of any isospin-3/2 resonance, $R^{(3)}$, are equivalent for proton and neutron targets, so that $\mathcal{A}(\gamma n \to R^{(3)0}) = \mathcal{A}(\gamma p \to R^{(3)+})$. Because the amplitudes are linear combinations of the form factors, the proton and neutron electromagnetic form factors are therefore also equal, $C_i^{(n)} = C_i^{(p)}$, $i = 3, 4, 5$.

The weak vector form factors $C_i^V(Q^2)$ for the amplitude $\mathcal{A}(W^+ n \to R^{(3)+})$ are related to the electromagnetic form factors. For isospin-3/2 resonances, these in fact coincide,

$$C_i^V = C_i^{(n)} = C_i^{(p)}, \quad i = 3, 4, 5. \tag{2}$$

The amplitude for a proton target is related to the neutron amplitude by Clebsch-Gordan coefficients, $\mathcal{A}(W^+ p \to R^{(3)++}) = \sqrt{3}\mathcal{A}(W^+ n \to R^{(3)+})$.

The form factors $C_3^{(p)}$ and $C_4^{(p)}$ from Eq. (1) agree to within 5% with those obtained earlier under the assumption of magnetic dipole dominance. Because they are deduced from data for $Q^2 < 3.5$ GeV^2, their normalization and Q^2 dependence should be reliable in this region.

The axial form factors are obtained from PCAC,

$$C_5^A = \frac{1.2 D_A}{1 + Q^2/3M_A^2}, \quad C_6^A = M^2 \frac{C_5^A}{m_\pi^2 + Q^2}, \tag{3}$$

where $D_A = 1/(1 + Q^2/M_A^2)^2$ is the dipole term with the axial mass $M_A = 1.05$ GeV. For the other axial form factors, $C_{3,4}^A$, we use the relations

$$C_4^A(Q^2) = -\tfrac{1}{4} C_5^A(Q^2) \quad \text{and} \quad C_3^A = 0, \tag{4}$$

suggested by dispersion relations [27,28].

The $P_{33}(1232)$ resonance is known to be dominant for low-energy neutrino scattering. The higher-mass resonances are very small for $E_\nu < 1.5$ GeV and produce a noticeable peak in the invariant mass distribution for $E_\nu > 2$–3 GeV. The second peak is produced primarily by the D_{13} and S_{11} resonances.

2. $D_{13}(1520)$ resonance

Among the isospin-1/2 resonances, $R^{(1)}$, the $D_{13}(1520)$ gives the dominant contribution in the second resonance region. The proton form factors in this case differ from those of neutrons. The vector part of the weak amplitude can be related to the electromagnetic amplitudes by isospin symmetry,

$$\mathcal{A}^V(W^+ n \to R^{(1)+}) = \mathcal{A}(\gamma n \to R^{(1)+}) - \mathcal{A}(\gamma p \to R^{(1)+}). \tag{5}$$

Similarly, the weak vector form factors can be related to electromagnetic ones via

$$C_i^V = C_i^{(n)} - C_i^{(p)}, \quad i = 3, 4, 5. \tag{6}$$

The Q^2 dependence of the vector form factors (for $Q^2 < 3.5$ GeV^2) was determined in Ref. [25] from precise electromagnetic data from JLab in the second resonance region [29–31],

$D_{13}(1520)$:

$$C_3^{(p)} = \frac{2.95 D_V}{1 + Q^2/8.9M_V^2}, \quad C_4^{(p)} = \frac{-1.05 D_V}{1 + Q^2/8.9M_V^2}, \quad C_5^{(p)} = -0.48 D_V, \quad C_3^{(n)} = \frac{-1.13 D_V}{1 + Q^2/8.9M_V^2}, \quad C_4^{(n)} = \frac{0.46 D_V}{1 + Q^2/8.9M_V^2}, \quad C_5^{(n)} = -0.17 D_V, \tag{7}$$

for protons and neutrons, respectively.

The normalization of the axial form factors is determined by PCAC and decay rates of the resonances. Unfortunately, their Q^2 dependence cannot be determined from the available data. In practice, we therefore consider two cases: (i) "fast falloff," in which the Q^2 dependence is the same as for the P_{33} resonance,

$$C_5^A = \frac{-2.1 D_A}{1 + Q^2/3M_A^2}, \qquad C_6^A = M^2 \frac{C_5^A}{m_\pi^2 + Q^2} \text{ ("fast falloff")}, \tag{8}$$

and (ii) "slow falloff," in which the Q^2 dependence is flatter and has the same form as that for the vector form factors for each resonance,

$$C_5^A = \frac{-2.1 D_A}{1 + Q^2/8.9M_A^2}, \qquad C_6^A = M^2 \frac{C_5^A}{m_\pi^2 + Q^2} \text{ ("slow falloff")}. \tag{9}$$

The other two form factors, $C_{3,4}^A$, are unknown, and for simplicity we set them to zero, $C_3^A = C_4^A = 0$.

3. $P_{11}(1440)$ and $S_{11}(1535)$ resonances

The two lowest-lying spin-1/2 resonances, $P_{11}(1440)$ and $S_{11}(1535)$, both have isospin $I = 1/2$. Their electromagnetic interaction depends only on two nonzero form factors, g_1 and g_2. For the proton these are determined for $Q^2 < 3.5$ GeV^2 from electroproduction helicity amplitudes, in analogy with the D_{13} resonance,

$$P_{11}(1440): g_1^{(p)} = \frac{2.3 D_V}{1 + Q^2/4.3M_V^2}, \qquad g_2^{(p)} = -0.76 D_V \left[1 - 2.8 \ln\left(1 + \frac{Q^2}{1\ \text{GeV}^2}\right)\right], \tag{10}$$

and

$$S_{11}(1535): \quad g_1^{(p)} = \frac{2.0 D_V}{1 + Q^2/1.2M_V^2}\left[1 + 7.2 \ln\left(1 + \frac{Q^2}{1\ \text{GeV}^2}\right)\right], \qquad g_2^{(p)} = 0.84 D_V \left[1 + 0.11 \ln\left(1 + \frac{Q^2}{1\ \text{GeV}^2}\right)\right]. \tag{11}$$

For the neutron case, if one neglects the isoscalar contribution to the electromagnetic current, one can use the relation $\mathcal{A}_{1/2}^{(n)} = -\mathcal{A}_{1/2}^{(p)}$. In this case the general relation in Eq. (6) between the weak and electromagnetic isovector form factors gives $g_i^V = -2g_i^{(p)}$, $i = 1, 2$.

The axial vector form factors of these two resonances are constrained by PCAC,

$$g_3^A = g_1^A \frac{M(M_R \pm M)}{Q^2 + m_\pi^2}, \tag{12}$$

with the $\pm$ corresponding to the P_{11} and S_{11} resonances, respectively. At $Q^2 = 0$ the couplings are also determined from PCAC and the elastic vertex of the resonance decay, which is known from experiment,

$$P_{11}(1440): \quad g_1^A(Q^2) = \frac{-0.51 D_A}{1 + Q^2/3M_A^2} \text{ ("fast falloff")}, \qquad g_1^A(Q^2) = \frac{-0.51 D_A}{1 + Q^2/4.3M_A^2} \text{ ("slow falloff")}, \tag{13}$$

and

$$S_{11}(1535): \quad g_1^A(Q^2) = \frac{-0.21 D_A}{1 + Q^2/3M_A^2} \text{ ("fast falloff")}, \qquad g_1^A(Q^2) = \frac{-0.21 D_A}{1 + Q^2/1.2M_A^2}\left[1 + 7.2 \ln \times \left(1 + \frac{Q^2}{1\ \text{GeV}^2}\right)\right] \text{ ("slow falloff")}. \tag{14}$$

B. Leading twist structure functions

The second set of inputs required for duality studies are the inclusive structure functions $F_1 = MW_1$, $F_2 = \nu W_2$, and $F_3 = \nu W_3$, which describe the DIS region. Here we summarize the relevant expressions for the structure functions in terms of leading twist parton distribution functions (PDFs). In practice we use several PDF parametrizations, namely from the GRV [32], CTEQ [33], and MRST [34] groups.

For electron scattering, the F_2 structure function of the nucleon, defined as the average of the proton and neutron structure functions, is given (at leading order in α_s and for three flavors), by

$$F_2^{eN} = \frac{1}{2}\left(F_2^{ep} + F_2^{en}\right) = \frac{5x}{18}\left(u + \bar{u} + d + \bar{d} + \frac{2}{5}s + \frac{2}{5}\bar{s}\right), \tag{15}$$

where the quark distributions are defined to be those in the proton. For neutrino scattering, the corresponding F_2 structure function is given by

$$F_2^{\nu N} = x(u + \bar{u} + d + \bar{d} + s + \bar{s}). \tag{16}$$

In the moderate and large-x region, where strange quarks are suppressed, the weak and electromagnetic F_2 structure functions approximately satisfy the "5/18 rule,"

$$F_2^{eN} \approx \frac{5x}{18}(u + \bar{u} + d + \bar{d}) \approx \frac{5}{18}F_2^{\nu N}. \tag{17}$$

The experimental confirmation of the factor 5/18 was indeed one of the important milestones in the acceptance of the description of DIS in terms of universal PDFs.

In the $Q^2 \to \infty$ limit, the F_1 structure function is related to F_2 via the Callan-Gross relation, $F_2 = 2xF_1$. Deviations from this relation arise due to perturbative α_s corrections, as well as from target mass effects and higher twists. It is sometimes convenient also to define the longitudinal structure

function F_L,

$$F_L = \left(1 + \frac{4M^2x^2}{Q^2}\right) F_2 - 2xF_1. \quad (18)$$

For large Q^2 the target mass term proportional to M^2/Q^2 can be omitted; however, at $Q^2 \sim$ few GeV^2 it can make an important contribution, especially at large x. Because the extraction of F_L requires longitudinal-transverse separation of cross-section data, which is challenging experimentally, in practice the F_L structure function is not very well determined. For F_L we use the parametrization of the MRST group [34]. To estimate the uncertainty in its determination, we consider two different scenarios for $2xF_1$, namely (i) Callan-Gross relation, $2xF_1 = F_2$, and (ii) the exact expression for $2xF_1$ from Eq. (18).

Finally, the charge-conjugation odd F_3 structure function for neutrino-nucleon scattering is given by

$$xF_3^{\nu p} = 2x(d - \bar{u} + s), \quad xF_3^{\nu n} = 2x(u - \bar{d} + s). \quad (19)$$

If one neglects the contribution of the strange quarks, $s \approx 0$, which is the case we consider here, the isoscalar $F_3^{\nu N}$ structure function is given simply by the valence u_v and d_v distributions:

$$xF_3^{\nu N} \approx x[(u - \bar{u}) + (d - \bar{d})] = x(u_v + d_v). \quad (20)$$

In the large-x region, where contribution of all sea quarks is very small, the F_2 structure function will also be proportional to xF_3,

$$xF_3^{\nu N} \approx F_2^{\nu N} \approx \tfrac{18}{5} F_2^{eN}. \quad (21)$$

In the next section we consider duality both for the total structure function and for the valence-only structure function. In the context of "two–component duality" [35], the resonance contributions are taken to be dual to valence quarks, whereas the nonresonant background is dual to the sea. In the resonance region, and especially at low Q^2, it may be reasonable that a resonance-based model of structure functions would generate a valencelike scaling function. Indeed, there were strong suggestions of such resonance-valence duality in the recent proton F_2 data from JLab [4]. In the present study we test the "two-component" duality hypothesis by comparing the calculated resonance structure functions with both the total and valence-only structure functions.

In the next section we use the above expressions to quantify the degree to which the averaged resonance structure function duals the leading twist structure functions for neutrino scattering and compare this with duality for the electron case.

III. DUALITY IN ELECTRON AND NEUTRINO STRUCTURE FUNCTIONS

A. Electron scattering

Before proceeding with the discussion of duality in neutrino scattering, we first consider duality for the better-known case of electron scattering. Recent high-precision experiments at Jefferson Lab and elsewhere [4–11] have allowed accurate tests to be performed of Bloom-Gilman duality in electron scattering. For the proton F_2 structure function, Niculescu *et al.* [4] found that the structure function in the resonance region, averaged over several intervals of x corresponding to the prominent resonance regions, reproduces well the scaling structure function down to relatively low values of Q^2. Our aim here is not necessarily to reproduce accurately the data with our resonance model [23–25] but rather to use phenomenological information on transition form factors to compare the workings of duality for neutrinos and electrons.

The isoscalar nucleon structure function $F_2^{eN} = (F_2^{ep} + F_2^{en})/2$, calculated as a sum of electroproduced resonances, is displayed in Fig. 1 as a function of the Nachtmann variable $\xi = 2x/\sqrt{1 + 4M^2x^2/Q^2}$ for several values of Q^2 from 0.2 to 2 GeV^2. The use of the Nachtmann variable takes into account kinematical target mass corrections, which can be important at large x and low Q^2. The prominent peaks correspond to the $P_{33}(1232)(\Delta)$ resonance at the largest ξ values in each spectrum. The next peaks, at smaller ξ, correspond to the second resonance region, where the $S_{11}(1535)$ and $D_{13}(1520)$ resonances dominate, and the $P_{11}(1440)$ resonance gives a small contribution. With increasing Q^2, the resonance peaks decrease in height and move to larger ξ.

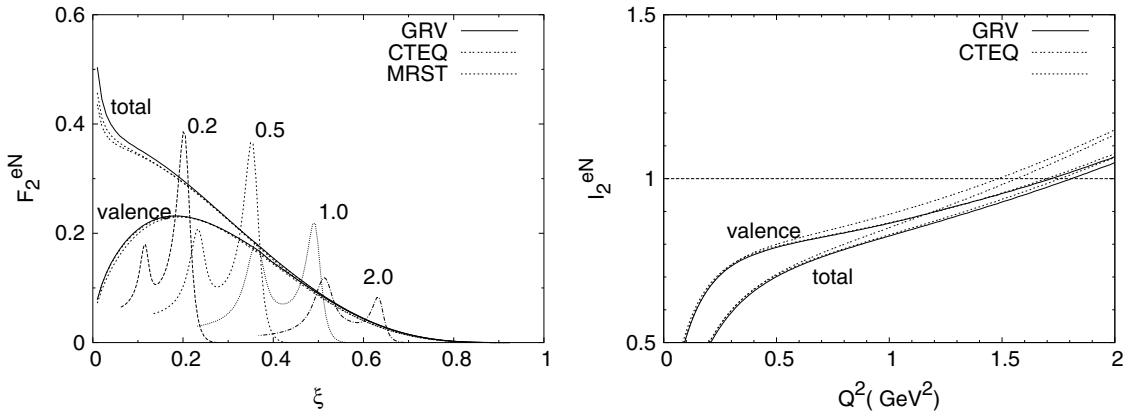

FIG. 1. Duality for the isoscalar nucleon F_2^{eN} structure function. (Left) F_2^{eN} as a function of ξ for $Q^2 = 0.2, 0.5, 1$, and 2 GeV^2 (indicated on the spectra), compared with several leading twist parametrizations [32–34] (valence and total) at $Q^2 = 10$ GeV^2. (Right) Ratio I_2^{eN} of the integrated F_2^{eN} in the resonance region to the leading twist functions (valence and total).

To examine the extent to which "local duality" works, we compare the ξ and Q^2 dependence of the individual resonances with the ξ dependence of the leading twist F_2^{eN} structure function, for both the total and the valence-only cases. For the latter, we use leading twist PDFs at $Q^2 = 10$ GeV^2 from the GRV [32], CTEQ [33], and MRST [34] groups. On average the resonances appear to oscillate around and slide down the leading twist function, reminiscent of the general features of the data as a function of ξ and Q^2; see Refs. [4,21]. For the calculated structure function, we consider the four resonances mentioned above and integrate over the invariant mass W of the final state in the region

$$1.1 \leqslant W \leqslant 1.6 \text{ GeV}, \tag{22}$$

where the upper bound covers the range of the resonances taken into account in this analysis.

The degree to which local duality is valid can be quantified by considering the ratio of integrals of the resonance (res) and leading twist (LT) structure functions,

$$I_i(Q^2) = \frac{\int_{\xi_{\min}}^{\xi_{\max}} d\xi \, \mathcal{F}_i^{(\text{res})}(\xi, Q^2)}{\int_{\xi_{\min}}^{\xi_{\max}} d\xi \, \mathcal{F}_i^{(\text{LT})}(\xi, Q^2)}, \tag{23}$$

where $\mathcal{F}_i$ denotes $F_2, 2xF_1$, or xF_3, and the integration limits correspond to $\xi_{\min} = \xi(W = 1.6 \text{ GeV}, Q^2)$ and $\xi_{\max} = \xi(W = 1.1 \text{ GeV}, Q^2)$. The closer this ratio is to unity, the better the agreement with duality will be. Defining the ratio $I_i(Q^2)$ in terms of integrals over the Nachtmann scaling variable ξ instead of Bjorken x implicitly includes target mass corrections in the structure functions [36–38], which are important at large x and small Q^2. This is especially so for the F_L structure function, which is intrinsically small. An alternative approach would be to express the target mass corrected structure functions in terms of x and Q^2 [36] and perform the integrations over x [21]. For a first investigation of duality, and because we are mostly concerned about the relative differences between duality in neutrino and electron scattering, the integrals over ξ in Eq. (23) provide a sufficient test of integrated duality.

The ratio I_2^{eN} for electron scattering is shown in Fig. 1 (right panel). The results are similar to those of the empirical analysis of JLab proton data [4]. The integrated resonance contribution is smaller than the leading twist at low Q^2 but increases with increasing Q^2. For $Q^2 \gtrsim 1$ GeV^2, the ratio I_2^{eN} is within $\sim$20% of unity when using the total DIS structure function. However, for the valence-only structure function the ratio is within $\sim$20% of unity over a larger range, $Q^2 \gtrsim 0.5$ GeV^2. The better agreement of the resonance curve with the valence-only leading twist curve supports the notion of two-component duality [35], as observed in the JLab F_2^{ep} data [4]. In more refined treatments one would also take into account the Q^2 evolution of the leading twist structure function. This will modify the quantitative behavior of the ratio with respect to Q^2 but not its essential features.

The fact that $I_2^{eN} < 1$ in our model can be understood from the fact that only the first four resonances are included in the structure function. Because F_2 is positive, the contribution from higher resonances as well as the nonresonant background increases the numerator in the ratio I_2^{eN} and thus improves the accuracy of duality. The behavior of the ratio I_2^{eN} at large Q^2 is less well constrained due to the current poor knowledge of the leading twist structure function at high x and of the transition form factors at large Q^2.

Recently, new high-precision data from Jefferson Lab have allowed longitudinal-transverse separations to be performed, which have enabled the proton $2xF_1$ structure function to be accurately determined at large x [7]. This has made it possible for the first time to perform quantitative tests of duality for the F_1 (or F_L) structure function. In Fig. 2 (left panel) we plot the isoscalar nucleon structure function $2xF_1^{eN}$, calculated for the above-mentioned four resonances, and compare with the leading twist parametrization from Ref. [34] at $Q^2 = 10$ GeV^2. The two leading twist curves correspond to the two scenarios for $2xF_1$ discussed in Sec. IIB, namely using the Callan-Gross relation, $F_2 = 2xF_1$, and using the exact expression in Eq. (18). The difference between the two curves is relatively small at $Q^2 = 10$ GeV^2, so that one can use either in the comparison with the resonance structure function.

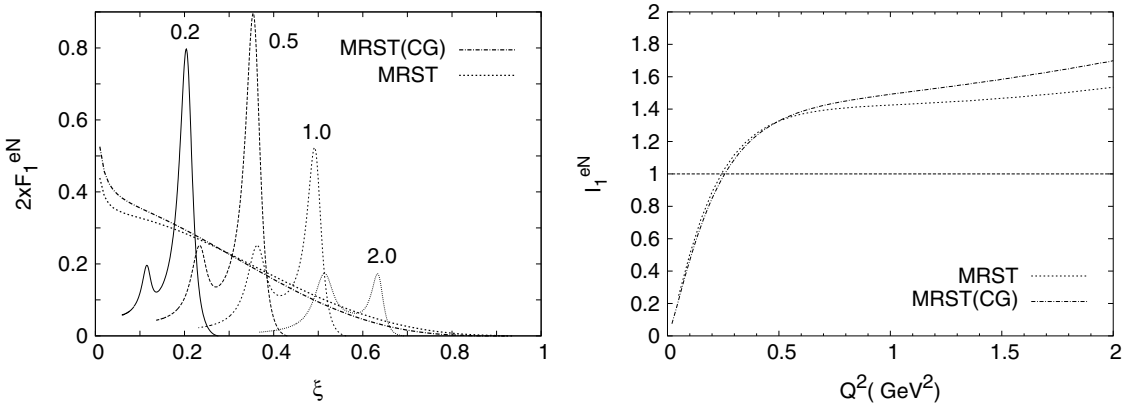

FIG. 2. Duality for the isoscalar nucleon $2xF_1^{eN}$ structure function. (Left) $2xF_1^{eN}$ as a function of ξ, for $Q^2 = 0.2, 0.5, 1$, and 2 GeV^2 (indicated on the spectra), compared with the MRST parametrization [34] at $Q^2 = 10$ GeV^2, using Eq. (18) (dotted) and the Callan-Gross (CG) relation, $F_2 = 2xF_1$ (dot-dashed). (Right) Ratio I_1^{eN} of the integrated $2xF_1^{eN}$ in the resonance region to the leading twist function [34] (see text).

With increasing Q^2, the resonance $2xF_1^{eN}$ structure function is seen to slide along the leading twist curve, just as in the case of F_2^{eN}, but on average sits slightly higher than the leading twist curve. This can be quantified by considering the ratio I_1^{eN}, defined in Eq. (23), which we plot in Fig. 2 (right panel). For most of the range of $Q^2 \gtrsim 0.5$ GeV^2 the ratio is some 30%–50% above unity, which may indicate the need for additional terms in the resonance sum. However, it is known that target mass corrections have a relatively larger effect on $2xF_1$ than on F_2 [21,36] and would tend to increase the leading twist functions, especially at large x (or ξ), and hence reduce the ratio I_1^{eN}.

B. Neutrino scattering

In the previous section we have demonstrated that the resonance model used here [25] reproduces the qualitative features of duality observed in electron scattering and have established the accuracy with which this duality holds in the model. Here we turn to the main aim of our article, which is to compare and contrast the workings of duality in eN scattering and in νN scattering. To make the comparison as rigorous as possible, we calculate the neutrino structure functions using the same four resonances as for the electron case, Figs. 1 and 2.

Neutrino interactions have particular features that distinguish them from electromagnetic probes. For the charge current reaction $\nu_\mu p \to \mu^- \Delta^{++}$, for example, only isospin-3/2 resonances are excited, and in particular the $P_{33}(1232)$ resonance. Because of isospin symmetry constraints, the neutrino-proton structure functions ($F_2^{\nu p}$, $2xF_1^{\nu p}$, and $xF_3^{\nu p}$) for these resonances are three times larger than the neutrino-neutron structure functions. In this case the resonance structure functions are significantly larger than the leading twist functions, $F_i^{\nu p(\mathrm{res})} > F_i^{\nu p(\mathrm{LT})}$, and quark-hadron duality is clearly violated for a proton target.

In neutrino-neutron scattering, in addition to isospin-3/2 resonances, all the isospin-1/2 resonances can also be excited. However, the total contribution of the three isospin-1/2 resonances considered here is smaller than that from the leading $P_{33}(1232)$ resonance. The leading twist curve for the νn structure functions lies above the resonance structure functions, $F_i^{\nu n(\mathrm{res})} < F_i^{\nu n(\mathrm{LT})}$, so that quark-hadron duality does not hold for this case either.

The general feature of the resonance curves is that at the onset of the resonance region, $W \lesssim 1.6$ GeV, the neutrino–proton structure functions are larger than the corresponding neutrino-neutron ones. However, in the deep inelastic region the structure functions are larger for neutrino-neutron scattering. It has been argued [13] for the case of electron scattering that for duality to appear one must sum over a complete set of even- and odd-parity resonances. In neutrino scattering, due to isospin symmetry constraints, duality will not hold locally for protons and neutrons separately, even if several resonances with both even and odd parities are taken into account [14]. In this case one can consider duality for the average of proton and neutron structure functions, which is the approach we take in this work. We demonstrate below that in this case duality holds with even greater accuracy than for electron scattering.

This discussion raises the question of how the transition occurs from the resonance to DIS regions in the case of neutrino scattering. We can speculate about the possible mechanisms of how this takes place. Starting from low W, the first resonance is the $P_{33}(1232)$, whose contribution to the νp structure function is three times larger than that to the νn, as mentioned above. To compensate its influence, this resonance must be followed by several isospin-1/2 resonances, which can contribute only to neutrino-neutron structure functions. This is what indeed happens—the $P_{11}(1440)$, $D_{13}(1520)$, and $S_{11}(1535)$ resonances are the next ones in the mass spectrum. In fact, the results of Ref. [25] show that the $P_{33}(1232)$ form factors fall steeply with increasing Q^2, whereas those for the $D_{13}(1520)$ and $S_{11}(1535)$ resonances fall slower, so that at $Q^2 \approx 2$ GeV^2 the two peaks are comparable. From our calculations we also know that with only these resonances the νn cross section (and structure functions) are still smaller than those of νp. Additional resonances with higher masses may also follow this trend and further enhance the νn structure functions to overcome those for νp.

At higher masses the isospin-3/2 resonances $P_{33}(1600)$ and $S_{31}(1620)$ appear, which also give three times larger contributions for νp scattering than for νn. They are again followed by the three isospin-1/2 resonances, $S_{11}(1650)$, $D_{15}(1675)$, and $F_{15}(1680)$, two of which have spin 5/2. Their contributions can be large due to the summation over six final spin states, which further increases the neutrino-neutron structure functions. One could suppose that in this region the neutrino-neutron contribution would exceed the neutrino-proton. Furthermore, we have again one isospin-3/2 resonance, the $D_{33}(1700)$, and three isospin-1/2 resonances—$D_{13}(1700)$, $P_{11}(1710)$, and $P_{13}(1720)$—to compensate its influence. Above $W = 1750$ MeV, and up to 2220 MeV, the isospin-3/2 resonances prevail, with 11 known states and only 9 with isospin 1/2.

A more detailed investigation of the interplay between the resonances with different spins would be possible after the form factors are determined for at least some of these higher-lying resonances. At present, however, we consider only the first four resonances, for which the νp cross section is always larger than the leading twist contribution, and the νn cross section is always smaller. This is one additional reason to compare only the average of the νp and νn structure functions.

The neutrino-nucleon $F_2^{\nu N}$ structure function is displayed in Fig. 3 (left panel) as a function of ξ for several values of Q^2. Here the $P_{33}(1232)$ resonance is seen as the largest peak at each Q^2. The next peak at lower ξ (larger W) is dominated by the $D_{13}(1520)$ and $S_{11}(1535)$ resonances. The contribution from the latter becomes more significant with increasing Q^2 because its form factors fall off more slowly than the dipole. The contribution of the $P_{11}(1440)$ resonance is too small to be seen as a separate peak. The two sets of resonance curves correspond to the "fast falloff" (lower curves) and "slow falloff" (upper curves) scenarios for the axial form factors discussed in Sec. IIA. The smooth curves are obtained from Eq. (16) using the GRV [32] and CTEQ [33] leading twist parton distributions at $Q^2 = 10$ GeV^2, as in Fig. 1. Just as in the case of electron-nucleon scattering, with increasing Q^2 the resonances slide along the leading twist curve, which

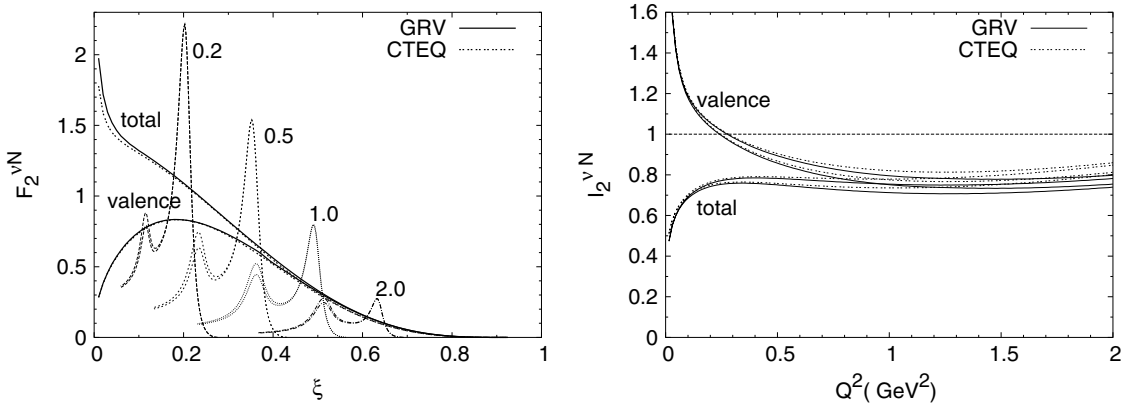

FIG. 3. Duality for the neutrino–nucleon $F_2^{\nu N}$ structure function. (Left) $F_2^{\nu N}$ in the resonance region at several Q^2 values (indicated on the spectra), compared with leading twist parametrizations [32,33] (valence and total) at $Q^2 = 10$ GeV^2. (Right) Ratio $I_2^{\nu N}$ of the integrated $F_2^{\nu N}$ in the resonance region to the leading twist functions [32,33] (valence and total). The upper (lower) resonance curves and the upper (lower) integrated ratios correspond to the "slow" ("fast") falloff of the axial form factors.

is required by duality. As in Fig. 1, we show both the total structure function and the valence-only contribution.

In Fig. 3 (right panel) we show the ratio of the integrals of the neutrino resonance and leading twist structure functions, defined in Eq. (23). The ratio is within ∼20%–25% of unity for $Q^2 \gtrsim 0.3$ GeV^2 and, unlike the corresponding electron-nucleon ratio I_2^{eN}, does not grow appreciably with Q^2. Again, the two sets of resonance curves correspond to the "fast falloff" (lower) and "slow falloff" (upper) scenarios for the axial form factors. The difference between the curves reflects the uncertainty in the calculation of $I_2^{\nu N}$. As expected, this ratio is close to 1 for the "valence-only" function at low Q^2, which favors the hypothesis of two-component duality [35]. A comparison for $Q^2 \lesssim 0.5$ GeV^2 may be questionable, however, because there the perturbative QCD expansion is unlikely to be valid. For large Q^2 the ratio is sensitive to the parametrization used for the leading twist curve, and the difference between the two parametrizations is smaller than the difference between the valence-only and total functions.

New features appear when considering the C-odd structure function $F_3^{\nu N}$. As discussed above for the case of $F_2^{\nu N}$, for the resonances considered here the proton $F_3^{\nu p}$ structure function is larger than the neutron $F_3^{\nu n}$, whereas for deep inelastic scattering the νn is larger. In our analysis we compare the isoscalar nucleon data, which are shown in Fig. 4 (left panel). As before, the lower and upper curves in the second resonance region correspond to the "slow" and "fast" falloffs of the axial form factors, respectively.

To quantify the degree to which the resonance and deep inelastic structure functions are dual, we calculate the ratio of integrals for the $xF_3^{\nu N}$ structure function as in Eq. (23). This ratio, shown in Fig. 4 (right panel), appears to fall off more rapidly with Q^2 than for the $F_2^{\nu N}$ ratio and reaches ∼0.7 at $Q^2 = 2$ GeV^2. The $F_3^{\nu N}$ structure function is in general more sensitive to the choice of axial form factors, and our results are consistent with the uncertainty in the axial form factors, which is estimated to be ∼30% at $Q^2 = 2$ GeV^2.

Finally, in Fig. 5 (left panel) we show the neutrino structure function $2xF_1^{\nu N}$ as a function of ξ for several Q^2 values. The resonance structure function are calculated for "slow falloff" and "fast falloff" axial form factors. The leading twist functions correspond to the MRST parametrization [34] using the Callan-Gross relation and the exact expression in Eq. (18). As in the electron-scattering case, the resonance contributions appear to lie above the leading twist curve for most of the range of ξ. The ratio $I_1^{\nu N}$, shown in Fig. 5 (right panel), is about 20% above 1 for $Q^2 > 1$ GeV^2, which again may be an indication that target mass effects need to be removed from the leading twist structure function before comparing with the resonance contributions.

C. Adler sum rule

One of the most fundamental results in neutrino scattering is the relation between the difference of the νn and νp structure functions for quasielastic (QE) scattering and for the rest of the higher mass states [39–41],

$$\left[g_{1V}^{(QE)}(Q^2)\right]^2 + \left[g_{1A}^{(QE)}(Q^2)\right]^2 + \left[g_{2V}^{(QE)}(Q^2)\right]^2 \frac{Q^2}{4M^2} + \int d\nu \left[W_2^{\nu n}(Q^2,\nu) - W_2^{\nu p}(Q^2,\nu)\right] = 2. \quad (24)$$

Because it measures the isospin of the target, this relation must hold for all values of Q^2.

In the $Q^2 \to 0$ limit, Eq. (24) is reduced to the Adler-Weisberger relation [39,40], which has been verified experimentally to good accuracy. For $Q^2 \neq 0$, it is known as the Adler sum rule [41], which has also been tested with data for neutrino deep inelastic scattering, and found to hold to ≈20% accuracy [42]. At large Q^2 it has a simple interpretation in the parton model, in terms of integrals of valence quark distributions. Using the model [25] for the resonance form factors, we can study how the Adler sum rule is satisfied as a function of Q^2.

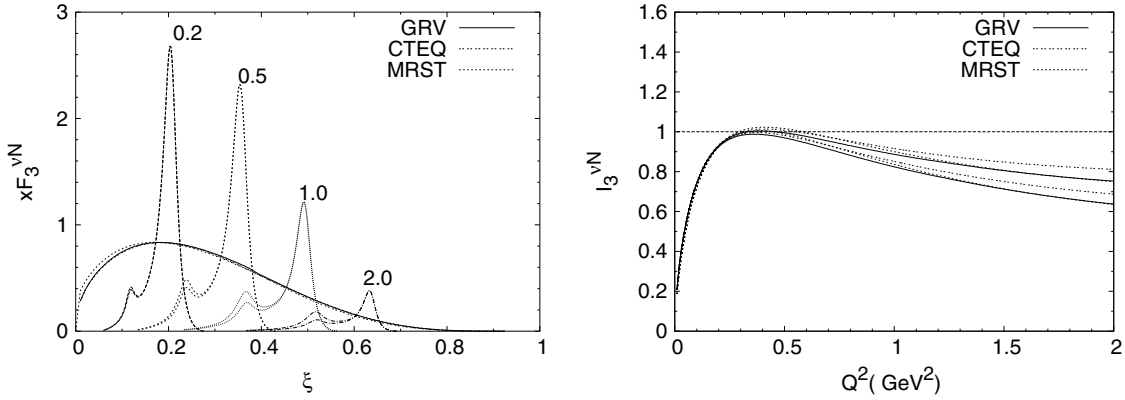

FIG. 4. Duality for the neutrino-nucleon $xF_3^{\nu N}$ structure function. (Left) $xF_3^{\nu N}$ in the resonance region for several Q^2 values, (indicated on the spectra), compared with several leading twist parametrizations [32–34] at $Q^2 = 10$ GeV^2. (Right) Ratio $I_3^{\nu N}$ of the integrated $xF_3^{\nu N}$ in the resonance region to the leading twist functions. The upper (lower) resonance curves and the upper (lower) integrated ratios correspond to the "slow" ("fast") falloff of the axial form factors.

For the QE form factors we use the following simple parametrization:

$$g_{1V}^{(QE)} = 1.0\, D_V, \quad g_{2V}^{(QE)} = 3.7\, D_V, \quad g_{1A}^{(QE)} = 1.23\, D_A. \quad (25)$$

The W_2 structure functions in Eq. (24) include contributions from resonance production and from the deep inelastic region. The resonance contribution is calculated for the first four resonances, as discussed earlier. The integration is performed in the range of $\nu_{\min} < \nu < \nu_{\max}$ corresponding to the final state mass range $1.1 < W < 1.6$ GeV. In terms of ξ, the integration of the structure function for each Q^2 corresponds to the area under the resonance curve from $\xi_{\min} = \xi(Q^2, W = 1.6\ \text{GeV})$ to $\xi_{\max} = \xi(Q^2, W = 1.1\ \text{GeV})$. The contribution from the remaining ξ interval, $0 < \xi < \xi_{\min}$, corresponds to the higher W region. For this we assume that the structure functions are given by the leading twist contributions, calculated from the MRST parametrization [34].

In Fig. 6 the individual contributions from the QE, resonance, and DIS regions are plotted as a function of Q^2. The (positive) QE contribution is large at low Q^2 but falls rapidly with increasing Q^2. The resonant piece of the sum is negative and partially cancels the QE component. The deep inelastic component grows with Q^2, because $\xi \to 1$ as $Q^2 \to \infty$, and for $Q^2 > 1$ GeV^2 contributes some 80% of the integral. Combining the three terms, the sum rule is found to be satisfied within ~10% over the whole range $0.5 < Q^2 < 2$ GeV^2.

Because the Adler some rule is based on very general grounds, one expects it to be exact. The 10% deviation of the calculated sum rule from the exact value should therefore be treated as an indication of the accuracy of the model. In practice, the uncertainty comes mainly from the axial form factors for the second resonance region and suggests that some of them are underestimated. The requirement that the Adler sum rule is satisfied exactly could therefore serve as a restriction on the currently unknown axial form factors.

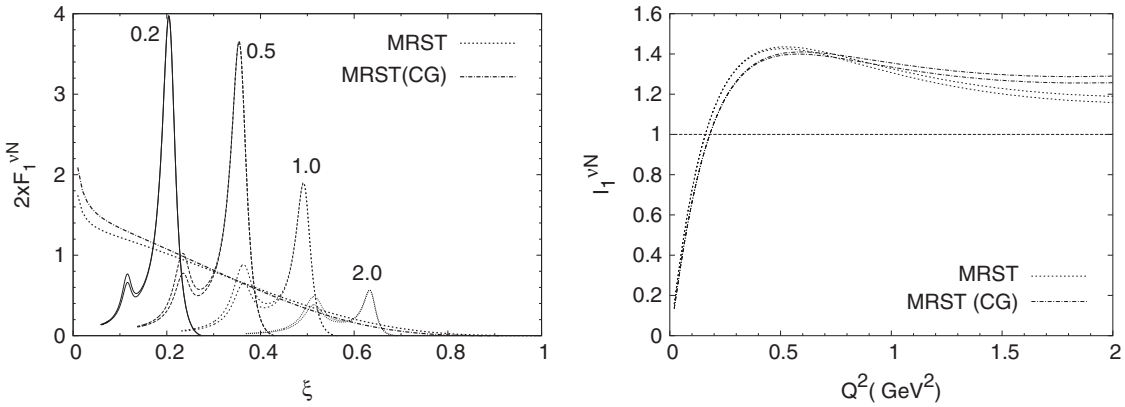

FIG. 5. Duality in the neutrino-nucleon $2xF_1^{\nu N}$ structure function. (Left) $2xF_1^{\nu N}$ in the resonance region at several Q^2 values (indicated on the spectra), compared with the MRST parametrization [34] at $Q^2 = 10$ GeV^2 using the exact expression in Eq. (18) (dotted) and Callan-Gross relation (dot-dashed). (Right) Ratio $I_1^{\nu N}$ of the integrated $2xF_1^{\nu N}$ in the resonance region to the leading twist function [34]. The upper (lower) resonance curves and the upper (lower) integrated ratios correspond to the "slow" ("fast") falloff of the axial form factors.

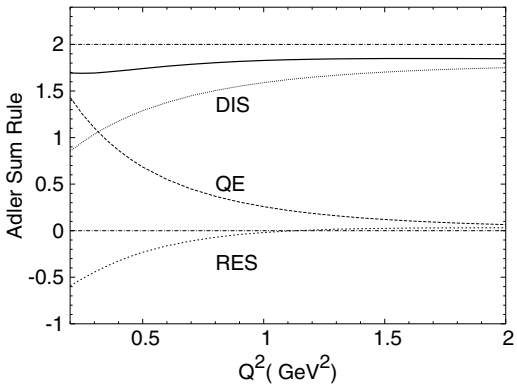

FIG. 6. Decomposition of the Adler sum, as a function of Q^2, into its QE (dashed), resonance (short dashed), and deep inelastic (dotted) contributions, as well as the total (solid).

IV. CONCLUSION

Motivated by the need to understand neutrino-nucleon cross sections in the $Q^2\sim$ few GeV^2 range, and the observation of quark-hadron duality in electron-nucleon scattering, we performed a detailed phenomenological study of duality in neutrino structure functions. Using a recently developed model [23–25] for the first four lowest-lying nucleon resonances, we computed the structure functions F_2, $2xF_1$, and xF_3 in the resonance region for proton and neutron targets and compared these with leading twist parametrizations.

As a check of the resonance model, we calculated the electron-nucleon structure functions and found that for each resonance these oscillate around the leading twist curves down to low values of Q^2, in qualitative agreement with duality. For quantitative comparisons, we defined ratios $I_i(Q^2)$ of resonance to leading twist structure functions, which in the ideal case of duality, should be unity. Our results show that for the F_2^{eN} structure function this ratio is below unity at low Q^2 and slowly grows with Q^2, consistent with recent experimental results [4]. The agreement with duality for $0.5 \lesssim Q^2 \lesssim 2$ GeV^2 in this case is at the level of 20%. At low Q^2 the resonance averaged F_2 structure function resembles valence quark distributions, apparently oblivious to sea quark effects, which supports the hypothesis of two-component duality [35]. For the $2xF_1$ structure function the ratio is about 40% above unity but would be reduced after correcting for target mass effects in the leading twist structure function.

For charged current neutrino scattering, duality does not hold for proton and neutron targets separately because of the dominant role played by the isospin-3/2 resonances. However, averaging over proton and neutron targets leads to large cancellations between $I = 3/2$ and $I = 1/2$ resonances, so that duality holds at the 20% level for isoscalar νN structure functions. Furthermore, the ratios $I_2^{\nu N}(Q^2)$ and $I_3^{\nu N}(Q^2)$ appear to reach constant values already for $Q^2 \approx 1$GeV^2.

Another interesting feature of our analysis is that the ratios $I_1^{eN}(Q^2)$ and $I_1^{\nu N}(Q^2)$ of the $2xF_1$ structure functions are consistently above unity. This may be an indication of the importance of target mass corrections in the leading twist F_1 structure functions, which are known to be more important than those in F_2.

In these comparisons we have used leading twist structure functions obtained from global parton distributions, which are well constrained by experimental data, especially for F_2. For the resonances, however, the data are very sparse, and theoretical input needs to be used. Our results therefore have an inherent uncertainty arising from poor knowledge of the transition form factors, particularly at high Q^2.

The results obtained here raise the following question: what is the most efficient and quantitative method for comparing the resonance contributions with the scaling curves and their QCD corrections? One approach is to compare the various contributions to sum rules, in which integrals over resonance and DIS contributions must reproduce physical constants. To this end we computed the various contributions to the Adler sum rule as a function of Q^2. This exercise shows how the relative contributions vary with Q^2 and saturate $\sim$90% of the sum rule. The remaining 10% could be accounted for by including more resonances and by better determining the transition form factors.

Overall, our quantitative study of neutrino reactions indicates that duality in structure functions, averaged over protons and neutrons, is expected to work to even better accuracy for neutrino scattering than for electron scattering.

ACKNOWLEDGMENTS

Authored by Jefferson Science Associates, LLC under U.S. DOE contract DE-AC05-06OR23177. The U.S. government retains a nonexclusive, paid-up, irrevocable, worldwide license to publish or reproduce this manuscript for U.S. government purposes. The financial support of BMBF, Bonn under contract 05HT 4 PEA/9 is gratefully acknowledged. E.A.P. and O.L. wish to thank Professor A. W. Thomas for hospitality in the Jefferson Lab Theory Center, where part of this work was carried out.

[1] E. D. Bloom and F. J. Gilman, Phys. Rev. Lett. **25**, 1140 (1970); Phys. Rev. D **4**, 2901 (1971) .
[2] A. De Rujula, H. Georgi, and H. D. Politzer, Ann. Phys. **103**, 315 (1977).
[3] X. Ji and P. Unrau, Phys. Rev. D **52**, 72 (1995) [arXiv:hep-ph/9408317].
[4] I. Niculescu *et al*., Phys. Rev. Lett. **85**, 1182 (2000); **85**, 1186 (2000).
[5] M. E. Christy, *Prepared for 9th International Conference on the Structure of Baryons (Baryons 2002), Newport News, Virginia, 3–8 Mar 2002*.
[6] J. Arrington, R. Ent, C. E. Keppel, J. Mammei, and I. Niculescu, Phys. Rev. C **73**, 035205 (2006).
[7] Y. Liang *et al*. (Jefferson Lab Hall C E94-110 Collaboration), JLAB-PHY-04-45 [arXiv:nucl-ex/0410027].
[8] F. R. Wesselmann *et al*. (RSS Collaboration), JLAB-PHY-06-518 [arXiv:nucl-ex/0608003].
[9] V. D. Burkert, AIP Conf. Proc. **603**, 3 (2001); T. A. Forest,

Prepared for 9th International Conference on the Structure of Baryons (Baryons 2002), Newport News, Virginia, 3–8 Mar 2002.
[10] N. Liyanage, JLAB-PHY-05-286; AIP Conf. Proc. **792**, 1019 (2005).
[11] A. Airapetian *et al*. (HERMES Collaboration), Phys. Rev. Lett. **90**, 092002 (2003).
[12] P. E. Bosted *et al*. (CLAS Collaboration), JLAB-PHY-06-517 [arXiv:hep-ph/0607283].
[13] F. E. Close and N. Isgur, Phys. Lett. **B509**, 81 (2001).
[14] F. E. Close and W. Melnitchouk, Phys. Rev. C **68**, 035210 (2003).
[15] N. Isgur, S. Jeschonnek, W. Melnitchouk, and J. W. Van Orden, Phys. Rev. D **64**, 054005 (2001).
[16] V. V. Davidovsky and B. V. Struminsky, arXiv:hep-ph/0205130.
[17] W. Melnitchouk, Phys. Rev. Lett. **86**, 35 (2001) [Erratum-*ibid*. **93**, 199901 (2004)].
[18] F. M. Steffens and K. Tsushima, Phys. Rev. D **70**, 094040 (2004).
[19] K. M. Graczyk, C. Juszczak, and J. T. Sobczyk, Nucl. Phys. Proc. Suppl. **159**, 241 (2006).
[20] K. Matsui, T. Sato, and T. S. Lee, Phys. Rev. C **72**, 025204 (2005).
[21] W. Melnitchouk, R. Ent, and C. Keppel, Phys. Rep. **406**, 127 (2005).
[22] D. Drakoulakos *et al*. (Minerva Collaboration), FERMILAB-PROPOSAL-0938, arXiv:hep-ex/0405002.
[23] E. A. Paschos, J. Y. Yu, and M. Sakuda, Phys. Rev. D **69**, 014013 (2004).
[24] O. Lalakulich and E. A. Paschos, Phys. Rev. D **71**, 074003 (2005).
[25] O. Lalakulich, E. A. Paschos, and G. Piranishvili, Phys. Rev. D **74**, 014009 (2006).
[26] Y. Hayato, Eur. Phys. J. C **33**, S829 (2004).
[27] S. L. Adler, Ann. Phys. **50**, 189 (1968).
[28] P. A. Zucker, Phys. Rev. D **4**, 3350 (1971).
[29] V. D. Burkert, R. De Vita, M. Battaglieri, M. Ripani, and V. Mokeev, Phys. Rev. C **67**, 035204 (2003).
[30] I. G. Aznauryan, V. D. Burkert, H. Egiyan, K. Joo, R. Minehart, and L. C. Smith, Phys. Rev. C **71**, 015201 (2005).
[31] I. G. Aznaurian, *Prepared for International Workshop on the Physics of Excited Baryons (NSTAR 05), Tallahassee, Florida, 10–15 Oct 2005*.
[32] M. Gluck, E. Reya, and A. Vogt, Eur. Phys. J. C **5**, 461 (1998).
[33] J. Pumplin, A. Belyaev, J. Huston, D. Stump, and W. K. Tung, J. High Energy Phys. 02 (2006) 032.
[34] A. D. Martin, R. G. Roberts, W. J. Stirling, and R. S. Thorne, Phys. Lett. **B604**, 61 (2004).
[35] H. Harari, Phys. Rev. Lett. **20**, 1395 (1969); **22**, 562 (1969); **24**, 286 (1970); Ann. Phys. **63**, 432 (1971); P. G. O. Freund, Phys. Rev. Lett. **20**, 235 (1968).
[36] H. Georgi and H. D. Politzer, Phys. Rev. D **14**, 1829 (1976).
[37] S. Kretzer and M. H. Reno, Phys. Rev. D **69**, 034002 (2004).
[38] F. M. Steffens and W. Melnitchouk, Phys. Rev. C **73**, 055202 (2006).
[39] S. L. Adler, Phys. Rev. **140**, B736 (1965).
[40] W. I. Weisberger, Phys. Rev. **143**, 1302 (1966).
[41] S. L. Adler, Phys. Rev. **143**, 1144 (1966).
[42] D. Allasia *et al*., Z. Phys. C **28**, 321 (1985).